JOURNAL OF MARITIME RESEARCH

Vol XXI. No. II (2024) pp 196–203

ISSN: 1697-4840, www.jmr.unican.es

Modeling Coastal Morphological Features in Proximity to Breakwaters Using Delft 3D

Mohamed M. Mirdan[1,*], Ehab R. Tolba[1], Elsayed M. Galal[1], Sherif Abdellaha[1]

ARTICLE INFO

Article history:
Received 25 Dec 2023;
in revised from 18 Jan 2024;
accepted 12 Mar 2024.

Keywords:
Hydrodynamics; Morpho Dynamics; Coastal Structures; Breakwaters; Numerical Modeling; Delft3D.

ABSTRACT

Coastal areas are crucial hubs within metropolitan regions, supporting diverse commercial and leisure activities. However, these ecosystems face threats from escalating natural calamities like storms and floods, disrupting local wave patterns and altering beach structures. Despite these challenges, the allure of coastal living fuels continuous urban expansion in these regions. To combat shoreline retreat caused by factors such as high tides, insufficient sediment movement, and strong waves, various protective structures are deployed. These measures aim to alleviate or prevent coastal erosion, although many were constructed without considering their environmental impact, economic implications, maintenance costs, or the potential widespread damage along the coastline. The strategic use of detached breakwaters as coastal defenses triggers changes in tombolo formations. This study explores the application of a Delft 3D model, a process-based tool, to examine the evolution of these morphological features, using a defined model domain from a prior case study. After conducting sensitivity analyses with optimized parameters like facua (set at 0.1), Chezy coefficient (at 60), and directional energy distribution, the model's outcomes are compared against empirical models. The Delft 3D simulations demonstrate the development of tombolos and salients 500 meters offshore after a 30-day simulation period for breakwaters positioned at distances of 150m, 200m, and 500m from the shoreline. This numerical analysis employing the Delft 3D model has enhanced our understanding of how the offshore distance of breakwaters impacts the evolution of coastal features such as tombolo and salient.

1. Introduction.

This Detached breakwaters, referred to as offshore breakwaters, are structures built parallel to the coastline, serving as vital defenses. They play a critical role in mitigating incoming wave energy, thereby creating sheltered areas by diminishing wave impact. Globally, these offshore breakwaters serve several engineering objectives: firstly, shielding water bodies from powerful waves; secondly, safeguarding beaches against erosion; thirdly, preventing the silting of harbor entrances; and finally, fostering shore growth for reclamation purposes. The implementation of these coastal structures leads to significant morphological alterations along the shoreline.

Breakwaters cause complex coastline changes. Sediment accretion or erosion behind the breakwater results from several hydrodynamic and morphologic processes. The hydrodynamic processes are what generate morphological changes, although morphological processes are of the most importance (Vlijm 2011a). When compared to other coastal constructions, detached breakwaters result in less erosion of the shoreline since they don't entirely prevent littoral drift and allow some drift material to flow through. The existence of coastal structures, such as detached breakwaters, can trap sand on their updrift sides, depleting the sediment budget and leading to beach erosion along nearby shorelines. It also provides a protected area where the wave energy is reduced and stops the incoming wave energy. When wave energy is reduced at the breakwater's lee

[1]Port said University, Faculty of Engineering, Civil Engineering Department.

[*]Corresponding author: Mohamed M.Mirdan. Tel. (+02) 01203143735. E-mail Address: Mohamed.mirdan@eng.psu.edu.eg.

side, sediment transport capacity is also reduced, and the sediment that is finally deposited forms a salient or tombolo (Razak and Nor 2018).

2. Delft3D model.

Utilizing numerical modeling proves to be an effective method for investigating hydrodynamic processes. This approach permits the examination of ongoing processes or specific design elements with relative ease under ideal conditions, offering a cost-effective alternative to extensive field-based or scaled model measurements.

The selection of a numerical model is influenced by various factors (Burcharth 2007), These factors encompass the required precision of wave or flow conditions, the essential physical processes to replicate, budget considerations, computation duration, and more. In response to these considerations, Deltares developed the software program Delft3D, which has gained prominence. Delft3D excels particularly in longer-term morphological time scales, effectively capturing significant hydrodynamic and morphological processes within reasonable processing time constraints (Deltares 2010). Its reliability has been demonstrated across a spectrum of coastal scenarios (Lesser et al. 2004a). The software employs a depth-averaged method, balancing computational efficiency with accurate outcomes (Johnson 2005).

2.1. Delft3D model description.

The Delft3D software package, version 4.04.01, constitutes a modeling system comprising multiple integrated modules. These modules operate collaboratively via a shared user interface to simulate various physical processes. The pivotal component within this suite is the Delft3D-Flow module, which serves as the primary module. To accurately replicate near-shore hydrodynamics, as illustrated in Fig. 1, the Delft3D-Flow module is coupled in real-time with the SWAN wave model. For an in-depth understanding of these modules, additional details can be found in the documentation provided by (Deltares 2010).

Figure 1: Online morphodynamic modeling scheme Delft3D.

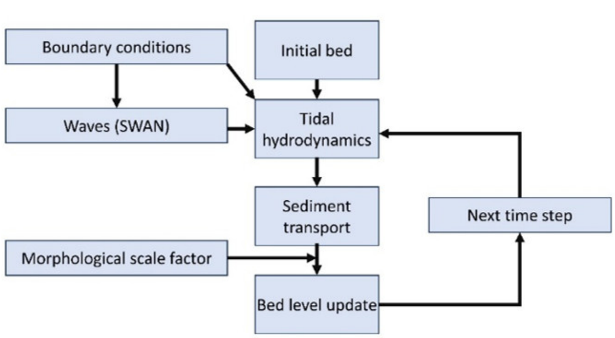

Source: Authors.

2.1.1. Delft3D-Flow.

The Delft3D-Flow module operates as a non-stationary, process-based numerical model. It tackles the Navier-Stokes equations applied to an incompressible fluid, incorporating Boussinesq assumptions along with shallow water approximations. Vertical accelerations are disregarded in this model, considering the hydrostatic pressure assumption in the vertical direction. Additionally, it employs an advection-diffusion equation to compute the transport of suspended sediment. For a detailed understanding of the governing equations utilized in this module, please refer to the sources provided by (Lesser et al. 2004b; Deltares 2010).

2.1.2. Delft3D-Wave.

Delft3D-WAVE, specifically SWAN operates as an Eulerian-based third-generation spectral wave model. SWAN functions by computing the evolution of wind-generated waves concurrently across different spatial points, relying on a two-dimensional wave action-density spectrum. With specific input parameters including bathymetry, wind, flow, and water level, SWAN can simulate wave propagation, wind-induced wave generation, nonlinear interactions among waves, and the dissipation of wave energy. Furthermore, wave-induced phenomena such as shear stresses and additional turbulence are factored into the flow computations through an online coupling of SWAN with Delft-3D-Flow.

2.1.3. Modeling approach.

The Delft3D-Flow module and SWAN are coupled online to allow for changes in bed level in wave calculations. (Vlijm 2011b). For the research modeling, a case study from (Razak and Nor 2018) is used as a reference case study.

2.1.4. Model scenarios.

The study focuses on a model test case featuring a solitary detached breakwater within a domain measuring 2100 meters by 790 meters. The incident waves approach the breakwater and shoreline perpendicularly. The breakwater maintains fixed dimensions: a length of 300 meters, width of 20 meters, and a height of 1.61 meters. The investigation into morphological changes in the proximity of this single detached breakwater utilizing the Delft3D model involves a series of numerical tests conducted over 30 days, as outlined in Table 1.

Table 1: Model scenarios tested on Delft3D.

Scenarios	Distance of the breakwater from the shore	Duration of the model simulation
I	150 m	30 days
II	200 m	30 days
III	300 m	30 days
IV	500 m	30 days

Source: Authors.

2.2. Delft3D flow set-up.

2.2.1. Grid.

Finite differences are the basis of the numerical model of Delft3D-FLOW.so There are two uniform cartesian grids in the Delft3D numerical domain: the FLOW and WAVE grids. The FLOW grid was utilized to solve the hydro-morphological evolution. covers an area of 2100x790 $\boldsymbol{m^2}$ in the alongshore and cross-shore directions, respectively. The WAVE grid, used for the wave's solver, covers an area of 4100x790 $\boldsymbol{m^2}$ in the alongshore and cross-shore directions, respectively. To avoid boundary issues, the WAVE grid is layered above the FLOW grid. The grid cell resolution of the flow grid is uniform and constant: $\Delta y = \Delta x = 10$ m, in the alongshore and cross-shore directions, respectively. As shown in Fig. 2.

2.2.2. Bathymetry.

A uniform alongshore bathymetry is employed to achieve a standardized and optimal representation. This bathymetry aligns with Dean's equilibrium profile in the cross-shore direction, maintaining a consistent offshore boundary depth of 12 meters. To incorporate the breakwater, local adjustments in the bathymetry are made based on design specifications like slope, crest width, and crest level. In the model setup, the initial bed profile slope is set at 1:50, and the profile shape remains linear across all distances from the breakwater to the shoreline, as illustrated in Fig. 3.

2.2.3. Time frame.

The Delft3D-Flow numerical model relies on finite differences, offering various schemes to discretize equations over time. In this context, explicit schemes are favored in numerical modeling due to their superior computational efficiency. Although faster than implicit schemes, explicit schemes maintain stability for shorter durations. To enhance the computational efficiency of implicit schemes, the Alternate Direction Implicit (ADI) method is employed. This method divides a single time step into two parts, aiding in improving computational effectiveness. Delft3D consistently solves each equation for both stages so that the spatial accuracy is at least in the second order. Although the implicit scheme is unconditionally stable, the Courant number should be kept smaller than a certain limit to ensure accuracy and efficiency in numerical computations.

$$c_f = 2\Delta t \sqrt{gH\left(\frac{1}{\Delta x^2}+\frac{1}{\Delta y^2}\right)} < 4\sqrt{2} \qquad (1)$$

In adherence to this time step restriction, a time step duration of 0.05 minutes is employed. The complete simulated duration for hydrodynamic modeling spans 30 days.

Figure 2: Flow grid and wave grid on Delft3D model.

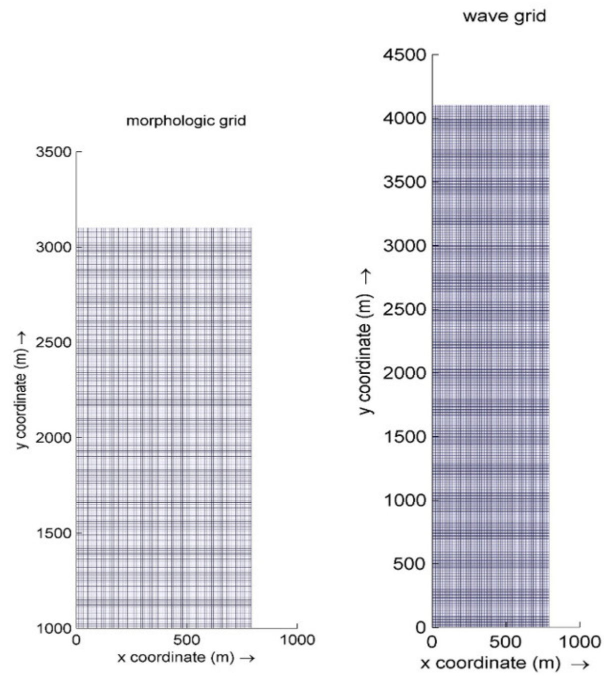

Source: Authors.

Figure 3: Bathymetry of five scenarios on Delft3D model; a) Plan, b) seabed elevation.

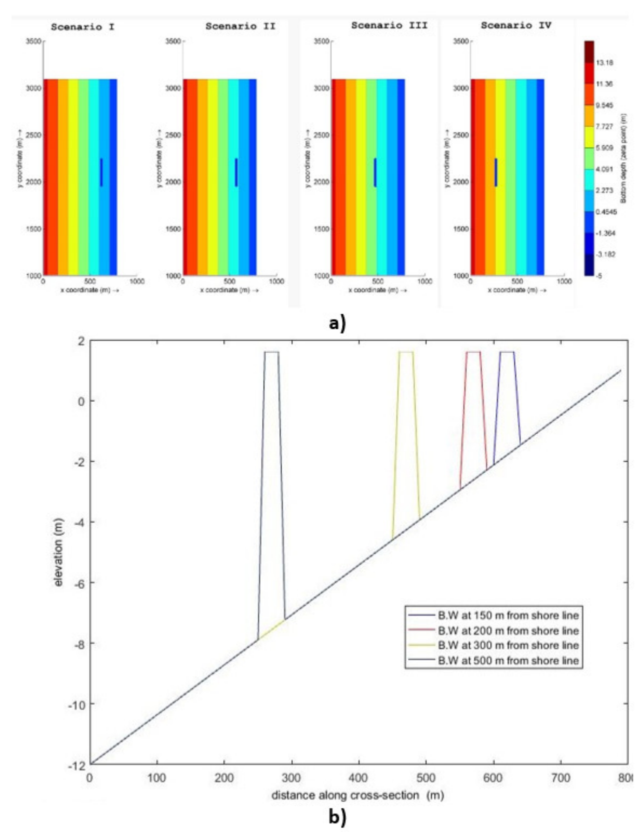

Source: Authors.

2.2.4. Processes and initial conditions.

In striving for a universally standardized approach, the focus is solely on sediments (constituents) and waves, omitting the consideration of wind effects. This is accomplished through online coupling with SWAN for the physical representation of waves. As for the initial conditions, both water level and sediment concentration are set at zero.

2.2.5. Boundary conditions.

The flow grid's Northern and Southern boundary conditions are established as Neumann boundaries, following the approach outlined by (Walstra and Roelvink 2004). Additionally, the offshore boundary to the West remains an open boundary in terms of water level, contributing to a well-defined and accurate formulation of the numerical model for the coastal system, as indicated by (Stelling 2009).

2.2.6. Physical parameters.

The physical parameters utilized for Delft3D-Flow are outlined and defined in Fig. 4.

2.2.7. Numerical parameters.

The numerical parameters utilized for Delft3D-Flow are outlined and defined in Fig. 5.

2.2.8. Additional parameters and output boundary conditions.

Two additional parameters are implemented for specific purposes within the model:

- Cstbnd #yes#: This parameter is set to prevent the formation of artificial boundary layers at the offshore boundaries, as recommended by (Deltares 2010).
- Msflux #false#: This parameter is employed to ensure satisfactory morphological outcomes. It involves the mass flow term, responsible for the sediment transfer directed onshore due to wave-induced effects, and it is initiated as specified.

Figure 4: Physical parameters on Delft3D flow model.

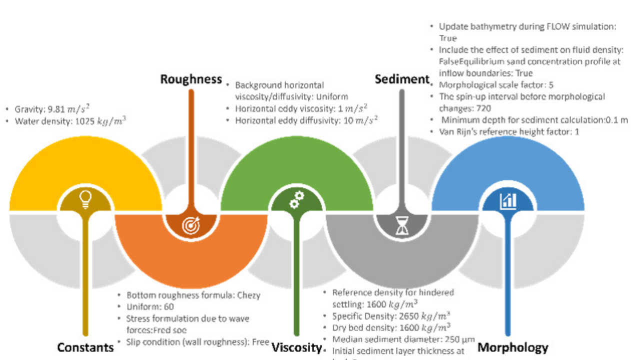

Source: Authors.

Figure 5: Numerical parameters on Delft3D flow model.

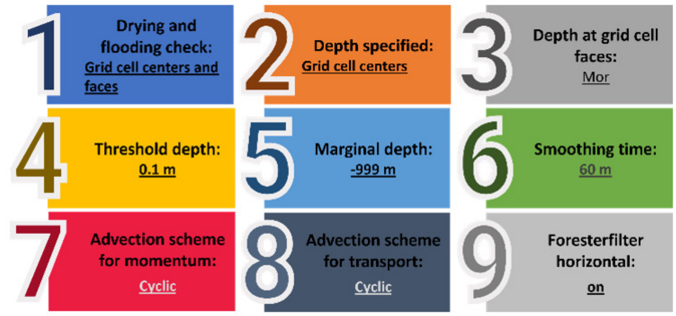

Source: Authors.

2.3. SWAN set-up.

2.3.1. Grid and bathymetry conditions.

A uniform and consistent wave grid is utilized, comprising 79 cells along the shore and 410 cells spanning along the shore. The resolution of each grid cell remains steady at $\Delta y = \Delta x = 10$ meters for the cross-shore and alongshore directions respectively. To enhance wave simulations, bathymetry incorporates boundary values and is derived from the flow grid, integrating with SWAN for flow-wave coupling. SWAN relies on water level, current, and bathymetric data sourced from Delft3D Flow results, as illustrated in Fig. 2 as previously defined.

2.3.2. Boundaries.

The JONSWAP spectrum, with a peak enhancement factor of 3.3, is employed for the offshore, Northern, and Southern boundaries. Directional spreading is achieved through the use of cosine and gamma functions. To establish consistent and unchanging boundary conditions in both time and space, specifications are set at a significant wave height (Hs) of 2.0 meters, a peak wave period (Tp) of 8 seconds, a wave direction perpendicular to the shore ($\theta = 270°$), and a directional spreading parameter of m=4.

2.3.3. Physical parameters.

The physical parameters utilized for Delft3D-SWAN are outlined and defined in Fig. 6.

Figure 6: Physical parameters Delft3D-SWAN model.

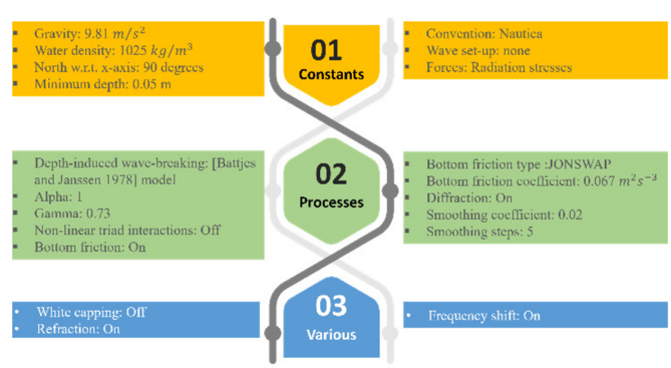

Source: Authors.

2.3.4. Numerical parameters.

The numerical parameters utilized for Delft3D-SWAN are outlined and defined in Fig. 7.

Figure 7: Numerical parameters Delft3D-SWAN model.

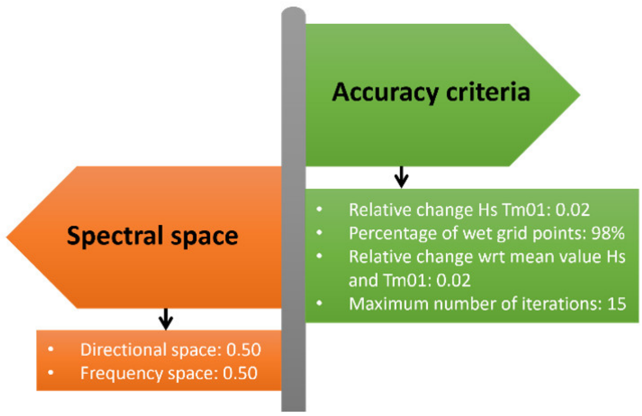

Source: Authors.

3. Model results.

In Scenario III, the gradual transformation of the tombolo is outlined step by step. This evolution occurs specifically when the breakwater is positioned 300 meters away from the shoreline, as depicted in Fig. 8.

The simulation of tombolo development spans across specific intervals: 0, 5, 10, 20, and 30 days. The initial point, T = 0 day, represents the state before any tombolo morphological changes occurred. Progressing to T = 5 days, the tombolo's morphological alterations begin as a result of wave refraction and diffraction within the breakwater's edges. This leads to the initial sediment formation at the protrusion. As the breakwater absorbs wave energy, the nearby coastal waves decelerate, enhancing the circulation of currents behind the structure and gradually accumulating sediment in the process. Continuing from T = 5 days, the silt accumulation advances noticeably by T = 10 days and further progresses by T = 20 days, gradually shaping into a sandbar. Finally, by T = 30 days, this sandbar fully connects the shoreline to the breakwater, completing the formation of the tombolo.

Figure 8: Numerical morphological evolution for scenario III (XB 300 m) for 30 days (results of Delft3D model).

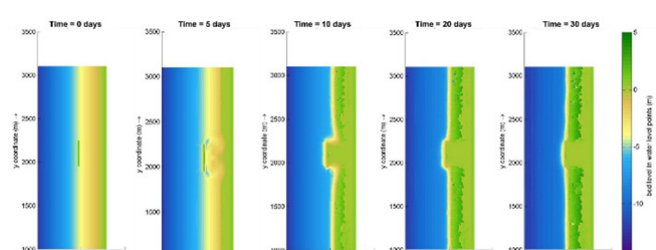

Source: Authors.

In the model, scenarios I, II, and III depict the evolution of a tombolo, while scenario IV demonstrates the formation of a salient, as illustrated in Fig. 9 and Fig. 10. The dissipation of wave energy leads to the accumulation of sediment in the sheltered region between the breakwater and the shoreline, a process triggered when waves encounter the detached breakwater. This phenomenon generates accretion within the protected area. When the breakwater is positioned closer to the beach and the tombolo-covered zone collects sediment from the swash impact, a significant portion of this sediment originates from the breakwater's edges. The alteration in wave height triggers the formation of small swirling currents on the sheltered side of the breakwater. These currents agitate the sediment due to wave action, leading to the creation of sizable scour holes.In scenarios I, II, and III, where the breakwater distances are set at 150 m, 200 m, and 300 m respectively, this swirling movement generates a circulating current behind the breakwater. As the current swirls, it picks up sediment along its path, gradually forming the tombolo.

As the breakwater moves farther from the beach, the patterns of sediment accumulation undergo notable alterations. The distance between the breakwater and the shoreline influences both the impact and the quantity of sediment transferred when waves reach the sheltered area behind the breakwater. In scenario IV, where the breakwater is situated 500 meters offshore, diverse wave flows emerge, effectively trapping sediment from the nearby shore zone within the salient. This distance creates specific wave dynamics that facilitate the entrapment of sediment within the created salient.

Figure 9: Numerical morphological evolution for four scenarios (results of Delft3D model); a) after 10 days, b) after 30 days.

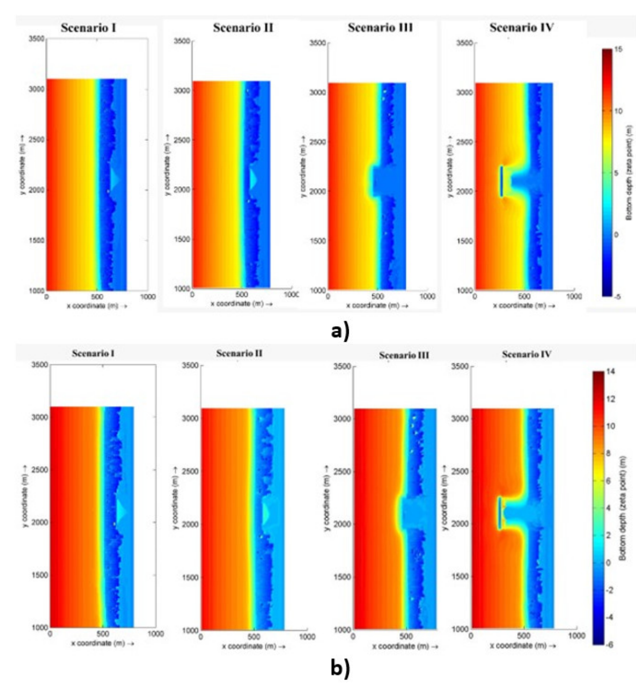

Source: Authors.

Figure 10: Simulated profile evolution initial and after 30 days for four scenarios (results of Delft3D model).

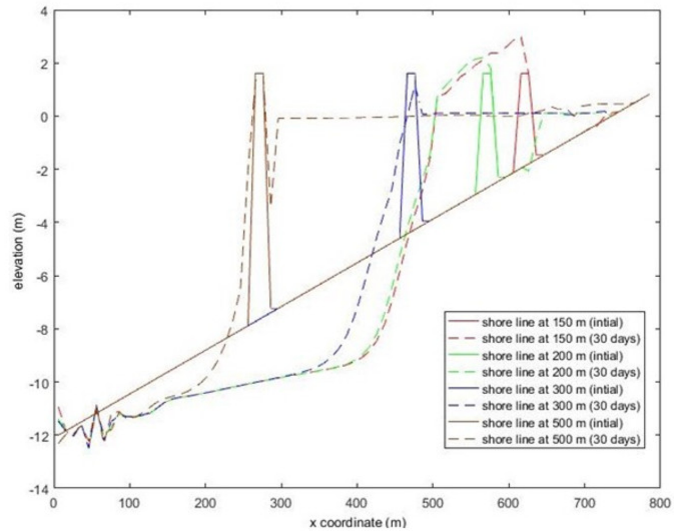

Source: Authors.

When the breakwater's length is greater than 0.8 times the distance between the shoreline and the breakwater, it results in the formation of a tombolo. Conversely, if the breakwater's length is shorter than 0.8 times that distance, it leads to the formation of a salient. This relationship between breakwater length and distance from the shoreline seems to determine whether a tombolo or a salient is formed in the simulated scenarios. The overall results of the Delft 3D simulation for all scenarios are summarized in Table 2.

Table 2: Delft 3D model results summary and categorization.

Scenarios	**Distance of the breakwater from the shore**	**Duration of the model simulation**	L_B/X_B	**Beach category simulated by Delft 3D**
I	150 m	30 days	2.00	Tombolo
II	200 m	30 days	1.50	Tombolo
III	300 m	30 days	1.00	Nearly tombolo
IV	500 m	30 days	0.60	Salient

Source: Authors.

3.1. Evaluating the Model Results in Contrast to Empirical Relationships.

The findings from the Delft 3D model align with the empirical relationships established by (GOURLAY 1981; C.T. Bishop 1982) when the ratio L_B/X_B equals or exceeds 2 and 1 respectively. However, they do not conform to the empirical relationship put forward by (Coastal Engineering Research Center 1984a; H. Noda 1984; Harris and Herbich 1986). Accordingly, Table3 summarizes this comparison.

Table 3: Ratio of breakwater length to breakwater distance from the shoreline $\frac{L_B}{X_B}$, of model results, compared to the tombolo evolution empirical relationships.

Ref.	**Relationship (tombolo formation)**	**150 m**	**200 m**	**300 m**
(GOURLAY 1981)	$\frac{L_B}{X_B} > 0.67\ to\ 1.00$	2.00	1.50	1.00
(C.T. Bishop 1982)	$\frac{L_B}{X_B} > 1.00$	2.00	1.50	1.00
(Coastal Engineering Research Center 1984b)	$\frac{L_B}{X_B} > 2.00$	2.00	1.50	1.00
(H. Noda 1984)	$\frac{L_B}{X_B} = 0.56$	2.00	1.50	1.00
(Harris and Herbich 1986)	$\frac{L_B}{X_B} > 1.00$	2.00	1.50	1.00

Source: Authors.

However, the formation of tombolo and salient concerning the various offshore distances of breakwater match the limiting conditions of (González and Medina 2001) as shown in Fig. 11, scenarios I, II, and III are categorized as tombolo because they are above the proposed limiting line of (González and Medina 2001), whereas scenario IV is categorized as salient as it is below the line. These empirical results completely match the model results produced by the Delft 3D model.

Figure 11: Determining Beach Categories in Accordance with (González and Medina 2001)and Evaluating the Delft 3D Model Results Across Various Scenario Cases.

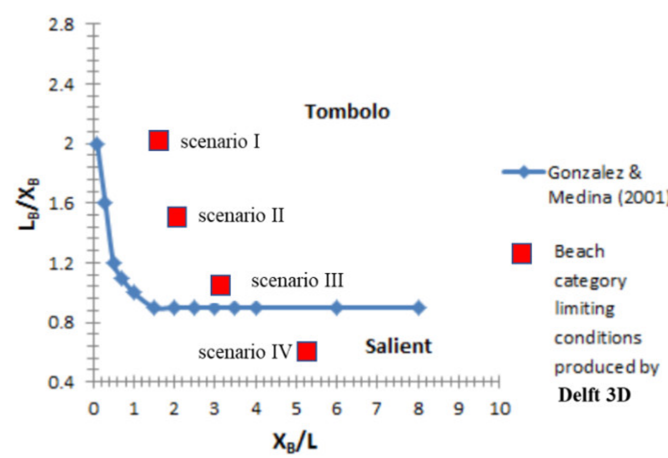

Source: Authors.

Despite the broad range of morphological change categories provided by the empirical relationship established by (J. Pope and J.L. Dean 1986), and supported by (Ahrens and Cox 1990), there's a significant disparity between the model's outcomes and the conceptual model they proposed. Their conceptual model suggests the formation of a salient rather than a tombolo at breakwater distances of 150 m, 200 m, and 300 m offshore, diverging from the conditions observed in this study. However, while not entirely aligning with the model conditions of this research, their conceptual model can serve as a general guideline for shoreline evolution.

The wave conditions in this study are presented as a hypothetical scenario (normal incidence wave), differing from the real wave circumstances. Despite this difference, the model's outcomes closely resemble those observed in the reference case study from literature (Ahmed 1997).Additionally, the assertion by (Edwards 2006) that the likelihood of tombolo formation increases with the distance of the breakwater from the offshore corroborates the results observed in this model.

Conclusions.

Over 30 days, the study utilized the process-based morphodynamic numerical model Delft3D to investigate the morphological changes in an alongshore uniform bathymetry with uniform grain size, influenced by a stationary oblique wave spectrum in the presence of a detached breakwater. By employing specific Delft3D parameters within the model domain, it becomes apparent that alterations in the shoreline behind a detached breakwater are influenced by both the breakwater's distance from the offshore and the characteristics of wave flows approaching the shoreline.

This investigation reveals multiple morphological transformations in the shoreline, notably including the formation of both tombolo and salient, which occur under varying offshore distances of the breakwater.

This study primarily focuses on numerically assessing the morphological impacts of constructing tombolo near coastal breakwater structures. As indicated by the Delft3D model outcomes, downdrift exerts the most consistent erosion influence on the beach.

In tombolo formation, downdrift often induces erosion regardless of parameter variations. However, in salient formation, downdrift is more likely to cause erosion and seldom leads to accretion. Moreover, the coastline on the updrift side is also affected by the detached breakwater. This impact results in fluctuations from accretion to erosion, contingent upon the breakwater's position relative to the shoreline and its ability to disperse wave energy. The magnitude and capabilities of the breakwater play a crucial role in determining these shoreline changes.

Both tombolo and noticeable siltation encounter fluctuations in sediment, experiencing both loss and accumulation. Comparatively, the updrift of tombolo formations undergoes erosion less frequently than that of salients.

In summary, the presence of a detached breakwater significantly influences wave energy dissipation and the creation of tombolos along the shoreline, contingent upon the breakwater's offshore distance. The Delft3D model adeptly depicts circulation patterns surrounding the structure and between it and the coastline. These patterns intricately influence the coastline's evolution.

Acknowledgements.

The authors will later thank the editors and reviewers for their efforts.

References.

Ahmed A (1997) 2D and 1D numerical model simulations for the effect of a single detached breakwater on the shore.

Ahrens JP, Cox J (1990) Design and Performance of Reef Breakwaters. J Coast Res 61–75.

Burcharth (2007) Environmental Design Guidelines for Low Crested Coastal Structures Elsevier Ltd.

Coastal Engineering Research Center (1984a) Shore Protection Manual. Shore Protection Manual I:1–337.

Coastal Engineering Research Center (1984b) Shore Protection Manual. Shore Protection Manual I:1–337.

C.T. Bishop (1982) A Review of Shore Protection by Headland Control. National Water Research Institute.

Deltares (2010) Delft3D-Flow. Deltares a:712.

Edwards BL (2006) Investigation of the effects of detached breakwaters at Holly Beach and Grand Isle, Louisiana. Geography and Anthropology M.S.

González M, Medina R (2001) On the application of static equilibrium bay formulations to natural and man-made beaches. Coastal Engineering - COAST ENG 43:209–225. https://doi.org-/10.1016/S0378-3839(01)00014-X.

GOURLAY MR (1981) Beach processes in the vicinity of offshore breakwaters and similar natural features. Coastal and Ocean Engineering 5.

H. Noda (1984) Depositional Effects of Offshore Breakwater Due to Onshore-Offshore Sediment Movement. In: Proceedings 19th Coastal Engineering Conference, ASCE, 2009-2025.

Harris MM, Herbich JB (1986) Effects of breakwater spacing on sand entrapment. Journal of Hydraulic Research 24:347–357. https://doi.org/10.1080/00221688609499313.

J. Pope and J.L. Dean (1986) Development of Design Criteria for Segmented Breakwaters. Coastal Engineering.

Johnson (2005) Modelling of waves and currents around submerged breakwaters. Coastal Engineering 52:10–11.

Lesser et al. (2004a) Development and validation of a three-dimensional morphological model.

Lesser GR, Roelvink DJA, van Kester J, Stelling G (2004b) Development and Validation of a Three-Dimensional Morphological Model. Coastal Engineering 51:883–915. https://doi.org-/10.1016/j.coastaleng.2004.07.014.

Razak MSA, Nor NAZM (2018) XBeach Process-Based Modelling of Coastal Morphological Features Near Breakwater. MATEC Web of Conferences 203:. https://doi.org/10.1051-/matecconf/201820301007.

Roelvink JAD, Walstra D-JR, van der Wegen M, Ranasinghe R (2016) Modeling of Coastal Morphological Processes BT - Springer Handbook of Ocean Engineering. In: Dhanak MR, Xiros NI (eds). Springer International Publishing, Cham, pp 611–634.

Stelling (2009) Computational modelling of flow and transport, CT4340 lecture notes, TU Delft.

Vlijm RJ (2011a) Process-based modelling of morphological response to submerged breakwaters. 235.

Vlijm RJ (2011b) Process-based modelling of morphological response to submerged breakwaters. 235.

Walstra and Roelvink (2004) Keeping it simple by using complex models. Advances in hydro-science and -engineering. 6th International conference on hydro-science 6.